

Lattice Dynamics and Phase Transitions of NiTi

M. Müllner, G. Herget, M. Keil, Universität Frankfurt, Institut für Kernphysik, Frankfurt, FRG

G. Eckold, Technische Hochschule Aachen, Institut für Kristallographie, Aachen, FRG

J.D. Suck, W. Weber, Kernforschungszentrum Karlsruhe, Institut für Nukleare Festkörperphysik, Karlsruhe, FRG

H. Jex, Universität Ulm, Institut für Festkörperphysik, Ulm, FRG

Phase Transitions

For the physical and microscopic understanding of the shape memory effect we have investigated the structures and lattice dynamics of nearly equiatomic NiTi by means of elastic and inelastic neutron scattering on single crystals and powdered samples (1-6).

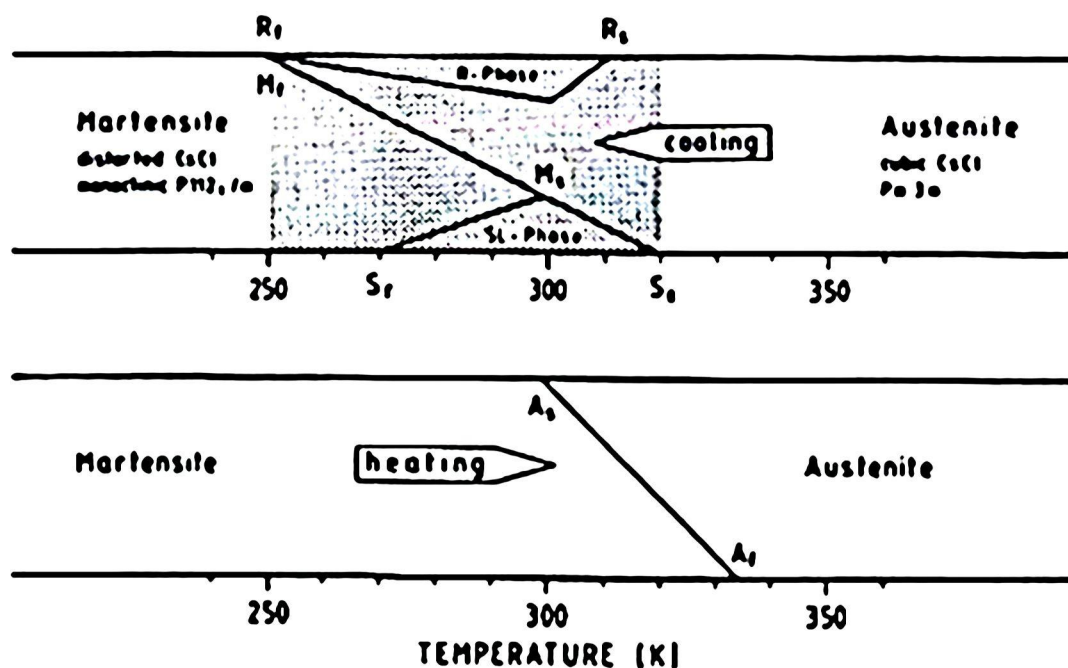


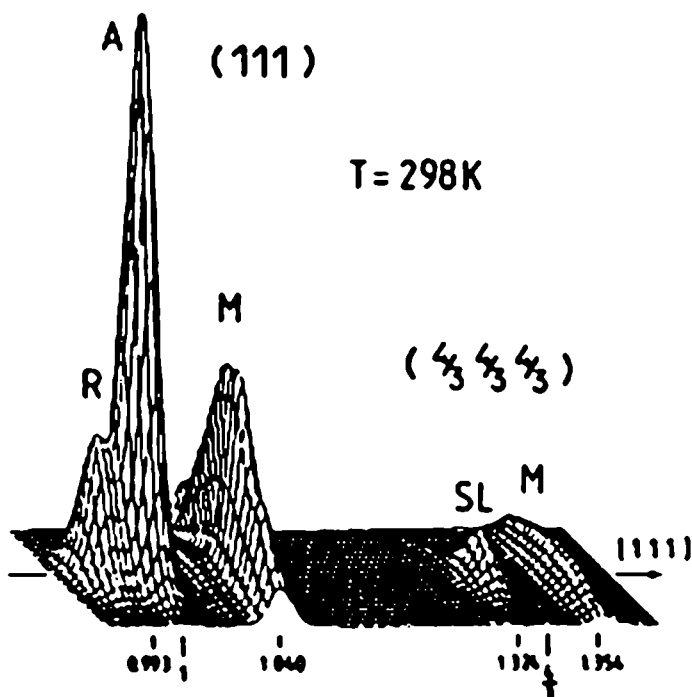
Fig. 1: Transformation behaviour of Ni₅₀Ti₅₀ on cooling and heating.

The transformation behaviour of Ni₅₀Ti₅₀ observed in a complete thermal cycle austenite (A) - martensite (M) - austenite is shown in Fig. 1. On cooling we find 3 phase transformations in an intermediate region (dotted area): first at 320 K superlattice (SL) reflections of the type 1/3(110) and 1/3(111) appear within the austenitic diffraction pattern at incommensurate positions. The splitting of the austenitic reflections at 310 K indicate the onset of a distorted R (rhombohedral)-phase, which is commensurate to the SL-phase. Martensitic reflections arise rapidly at 300 K. Simultaneously the SL- and R-reflections reach maximum intensity, which decreases considerable by lowering the temperature.

Upon heating we have a direct transformation from martensite to austenite without intermediate phases.

The overlap of all structural phases in the intermediate region between austenite and martensite is demonstrated in the diffraction pattern (Fig. 2) measured at 298 K. The M-reflections show

Fig. 2: Diffraction pattern of $\text{Ni}_{50}\text{Ti}_{50}$ in (111)-direction at 298 K.



an exceptional transversal broadening due to the orientational multiplicity of the structural domains in the martensitic phase. Detailed measurements of the SL-reflections in several Brillouin-zones (Fig. 3) show, that

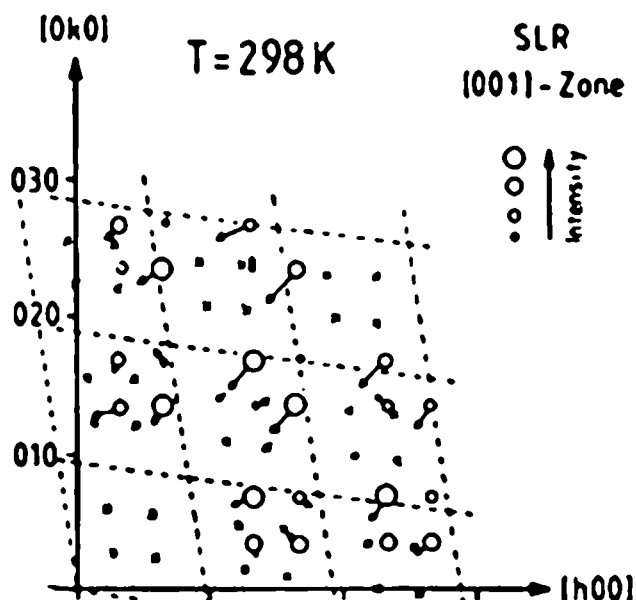
1. the shifts from the exact $1/3$ positions relative to the austenitic lattice are different,

2. not all of them become "locked-in" to the commensurate rhombohedral positions at lower temperature.

Similar results have been obtained on the ternary alloy $\text{Ni}_{50}\text{Ti}_{30}\text{Fe}_{20}$, by x-ray diffraction (7).

This two dimensional shift pattern is inconsistent with simple incommensurate wave models applying charge-density waves, but is well described by a modulated lattice relaxation model (8).

Fig. 3: q-dependent shifts of the SL-reflections related to the cubic $1/3$ positions (O). Dashed lines and crosses represent the rhombohedral lattice. The rhombohedral distortion is enlarged, the length of each arrow shows the amount of the shift.



Phonon Dispersion

The phonon dispersion relations for a single crystal of $\text{Ni}_{50}\text{Ti}_{50}$ were measured in the undistorted austenitic phase in the high symmetry directions $(\zeta 00)$, $(\zeta \zeta 0)$, $(\zeta \zeta \zeta)$ and $(\frac{1}{2}, \frac{1}{2}, \zeta)$ at 400 K by means of inelastic scattering of neutrons (Fig. 4). The single crystal (0.8 cm³ in volume, 0.4° mosaic-spread) has been grown by a Czochralski technique from a levitated melt (2,3).

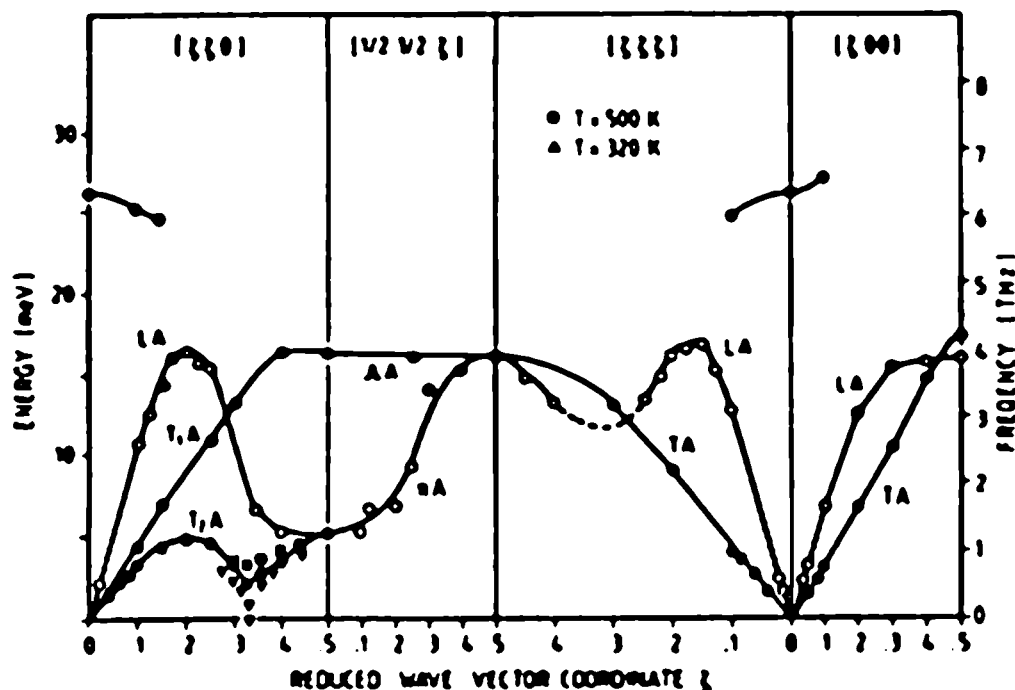


Fig. 4: Phonon dispersion of $\text{Ni}_{50}\text{Ti}_{50}$ at 400 K. Lines are only a guide for the eye.

Some general comments can be made concerning the observed phonon dispersion:

1. The transverse acoustic phonon branch in (110) -direction T_{2A} (polarisation along $(1\bar{1}0)$) indicates a softening at $q_{110} = q_{\max}/3$. By lowering the temperature towards $T_S = 320$ K this mode condenses to zero energy leading to the $1/3(110)$ type SL-reflections.

2. The considerable softening in the (111) longitudinal acoustic branch at $q_{111} = q_{\max}/3$, similar to the characteristic feature of bcc metals, may be related to anomalous and also normal self-diffusion processes.

3. The phonons in the energy region between 4 and 6 meV were found to be relatively poor defined.

4. The slopes of the phonon branches near $q = 0$ agree reasonable with elastic constants obtained by ultrasonic experiments (9).

5. The measurements of optical phonons turned out to be exceptionally difficult because of their extremely low intensities.

Phonon Density of States (PDOS)

The PDOS of a $\text{Ni}_{0.5}\text{Ti}_{0.5}$ powder sample was measured in the austenitic, martensitic and intermediate phase by means of inelastic neutron scattering for the first time (6). The phonon spectra are dominated by two pronounced peaks near 17 meV and at

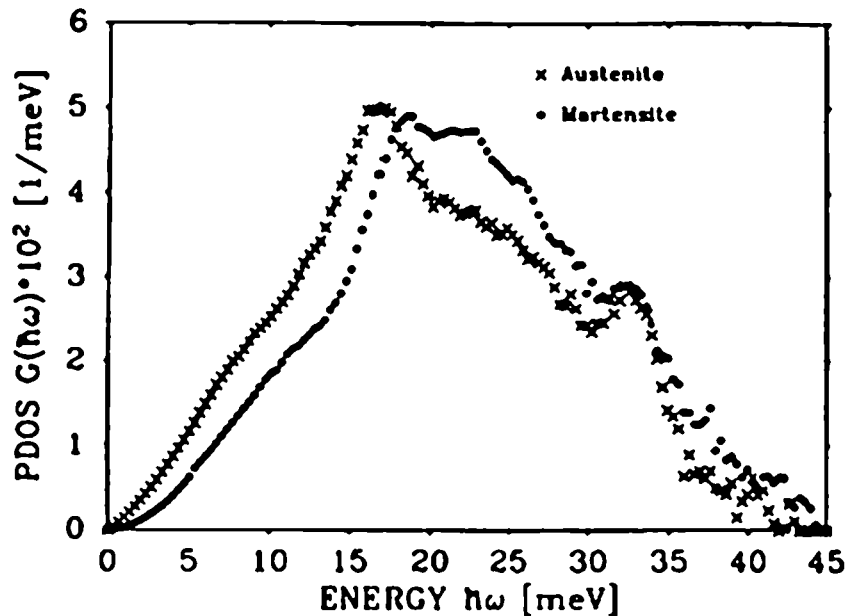


Fig. 5: Phonon density of states of $\text{Ni}_{0.5}\text{Ti}_{0.5}$ at 400 K (x) and 200 K (●).

33 meV (Fig. 5). Within experimental accuracy the PDOS of the austenitic and the intermediate phase are identical, but a strong hardening of predominantly acoustic phonons in the martensitic phase is observed.

In contrast to model calculations, based on fits to the measured phonon dispersion, we find no pronounced gap between the acoustic and the optic modes in the PDOS and also a considerable higher cutoff frequency of about 37 meV than expected from these calculations.

From the measured PDOS of $\text{Ni}_{0.5}\text{Ti}_{0.5}$ (Fig. 5) we computed the overall Debye-Waller factor (DWF) in the martensite and the austenite phase. The results (Fig. 6) are compared with the individual, isotropic DWF's of Ni and Ti. We obtained these data from our early neutron-diffraction experiments on a polycrystalline probe of nearly equiatomic NiTi, possibly with a large static lattice displacement due to the preparative treatment. The agreement of these DWF's from different experimental methods and samples is satisfactory. The cusp in the intermediate phase (dotted area) we associate with enhanced thermal vibration of the atoms and the static displacement in this soft-mode regime.

The calculation of the specific heat in the martensitic and austenitic phase of $\text{Ni}_{0.5}\text{Ti}_{0.5}$ from the PDOS-measurements are

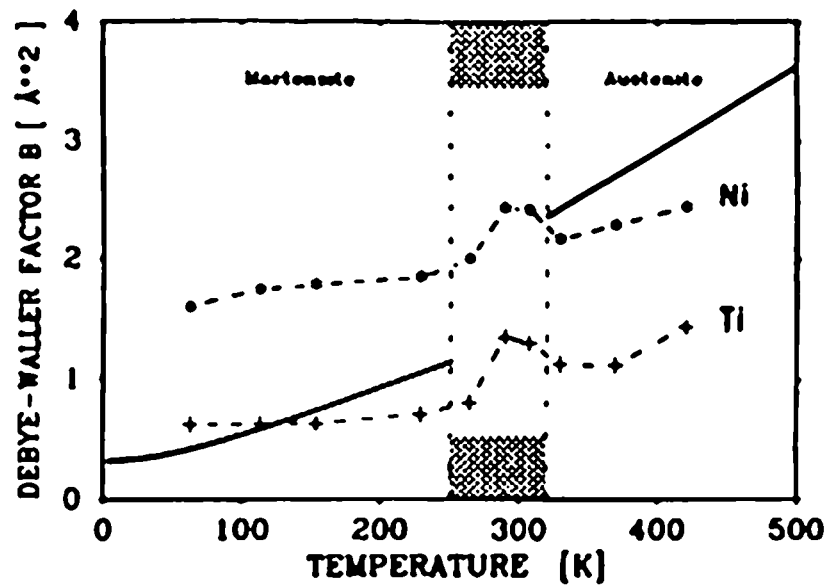


Fig. 6: Overall Debye-Waller factor (DWF) of $\text{Ni}_{0.5}\text{Ti}_{0.5}$ calculated from the PDOS measurements (—) compared with the individual DWF's from neutron diffraction experiments (1,2).

presented in Fig. 7. The results are compared with experimental data obtained from a $\text{Ni}_{0.9}\text{Ti}_{0.1}$ specimen with shifted stoichiometry, which increases the transition temperature (cf. the shifted peak position). The low temperature measurements agree very well, the deviation of the experimental values in the high temperature phase gives evidence for anharmonic contributions. Since our calculations hold only within the limits of the harmonic approximation we can not reproduce the anomalies of the DWF and the specific heat in the intermediate phase.

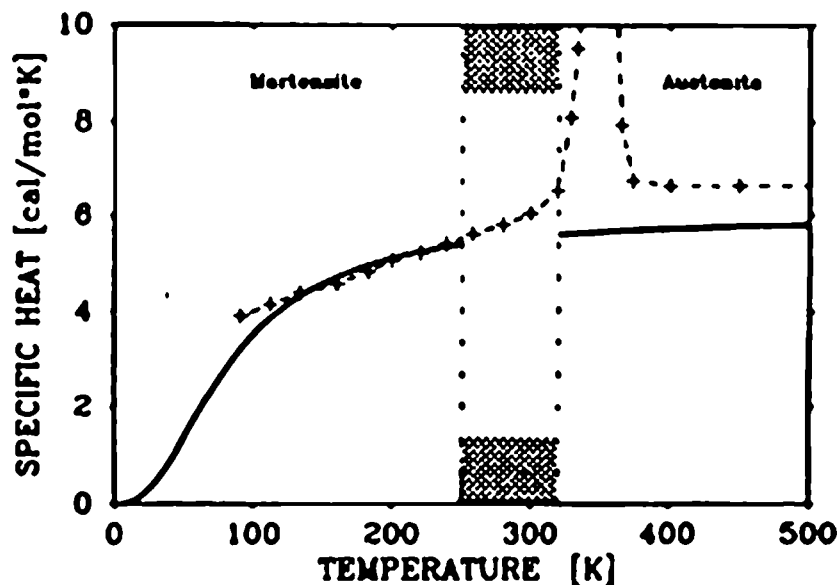


Fig. 7: Specific heat of $\text{Ni}_{0.5}\text{Ti}_{0.5}$ calculated from PDOS measurements (—) compared with experimental data (9).

Model Calculations

For the interpretation of our experimental results in lattice dynamics we applied the Born-von Kármán theory (BvK) as well as a method of Varma and Weber considering electron phonon coupling.

Born-von Kármán Theory

The calculated phonon dispersion relation of equiatomic NiTi using a BvK-model with interatomic forces between the second-nearest neighbour atoms is shown in Fig. 8.

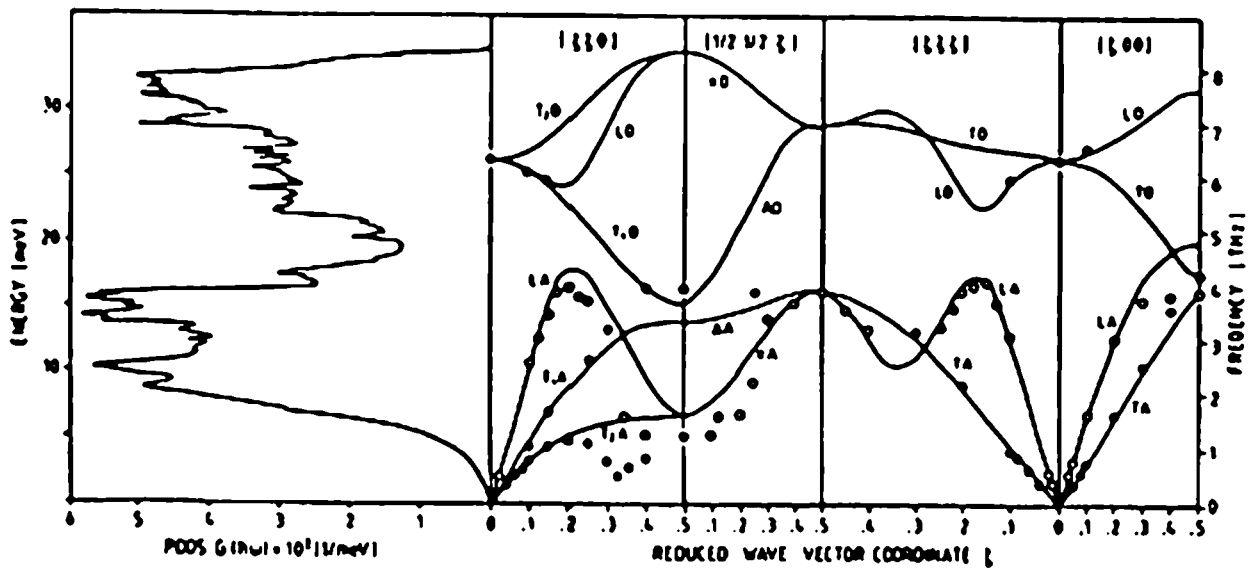


Fig. 8: BvK-fit of phonon dispersion for equiatomic NiTi to our experimental data (●○, cf. Fig.4) and the derived phonon density of states.

Since the BvK-model is purely phenomenological it does not provide a physical representation of the system. However, this model is adequate for projecting and optimizing of measurements as well as for computing the PDOS and related thermodynamic properties. From this point of view our experimental results are satisfactorily described by a BvK-model even with simple short-range forces. This method also has been used for computing the isotropic, overall DWF and the specific heat of stoichiometric NiTi in the austenitic phase. The results are in reasonable agreement with the data derived from the PDOS measurements (Fig. 6 and 7).

Electron-Phonon Interaction

On the atomistic level the lattice vibrations are determined by the electronic states near the Fermi-edge. The lattice dynamical behaviour of transition metal compounds predominantly is affected by d-electrons and conduction electrons. The characteristic features of the d-electrons are assumed to be responsible for anomalies found in the dispersion relation of a variety of those compounds. First principle calculations with electronic band structure contributions were successfully applied.

A first attempt to compute the electron phonon coupling in NiTi was made by Bruinsma (11), however, with inadmissible simplifications.

We used the complete theory of Varma and Weber (12) utilizing the derivation of the Hamiltonian in the electron-phonon matrix elements as well as the generalized susceptibility.

Our nonorthogonal tight binding fit to the results of an augmented plane wave calculation of Papaconstantopoulos (13) agrees very well with band structures and densities of electronic states in the literature (11,14).

Preliminary results of the phonon dispersion reproduce the softening of the [110] T_{2A} and the [111] LA mode (cf. Fig. 4). The calculations are in progress.

References

- (1) H. Tietze, M. Müllner, B. Renker:
J. Phys. C: Solid State Phys. 17 (1984) L529
- (2) H. Tietze: Thesis, University Frankfurt,
IKF-D347 (1984)
- (3) H. Tietze, M. Müllner, P. Selgert, W. Assmus:
J. Phys. F: Met. Phys. 15 (1985) 263
- (4) M. Müllner, H. Tietze, G. Eckold, W. Assmus:
Proc. Int. Conf. on Martensitic Transformations,
ICOMAT-86, Nara (Japan), edited by I. Tamura
(The Japan Inst. of Metals) 1987, p.159
- (5) G. Herget, M. Müllner, G. Eckold, H. Tietze, W. Assmus:
IKF Annual Report 1987, p.77-79
- (6) G. Herget, M. Müllner, J.B. Suck, R. Schmidt, H. Wipf:
to be published.
- (7) S.M. Shapiro, Y. Noda, Y. Fujii, Y. Yamada:
Phys. Rev. B 30 (1984) 4314
- (8) Y. Yamada, Y. Noda, M. Takimoto:
Solid State Comm. 55 (1985) 1003
- (9) O. Mercier, K.N. Melton, G. Gremaud, J. Hägi:
J. Appl. Phys. 51 (1980) 1833
- (10) R.J. Wasilewski, S.R. Butler, J.E. Hanlon:
Metal Sci. J. 1 (1967) 104
- (11) R. Bruinsma: Phys. Rev. B 25 (1982) 2951
- (12) C.M. Varma, W. Weber: Phys. Rev. B 19 (1979) 6142
- (13) D.A. Papaconstantopoulos, G.N. Kamm, P.M. Pouloupoulos
Solid State Comm. 41 (1982) 93
- (14) J.D. Shore, D.A. Papaconstantopoulos:
J. Phys. Chem. Solids 45 (1984) 439

This work was financially supported by the German Federal Minister for Research and Technology under contract No. BMFT 03-MU1FRA.